Electronic Supplementary Material (ESI) for Lab on a Chip.

Supporting Information for:

3D Printing of Liquid Metals as Fugitive Inks for Fabrication of 3D Microfluidic Channels

Dishit P. Parekh[1], Collin Ladd[1]*, Lazar Panich[1], Khalil Moussa[2] & Michael D. Dickey[1]*

[1]Department of Chemical and Biomolecular Engineering, North Carolina State University

[2]Senior Director, Materials R&D, 3D Systems Inc., Rock Hill, SC

*Contributed equally

Printing Process. The liquid metal printing was implemented using a customized 3D printer. The stage of the printer is a Minitech CNC machine with an X, Y, Z travel distance of 300 x 200 x 200 mm and a resolution of 10 µm. The speed used for printing was varied from 10 mm/min to 1200 mm/min with most of the samples made with a speed of 120 mm/min. The spindle on the CNC machine was replaced with a Nordson syringe and needle setup using a 3D printed adapter. The pneumatic pressure was provided using Ultimus™ V High Precision Dispenser from Nordson EFD. The forward pressure and the vacuum was adjusted depending on the hydrostatic head of the liquid metal in the syringe such that the liquid metal was sheared out from the needle tip rather than extruded out with net pressure in the range of 0.1-5 kPa. The needle standoff distance was in the range of 5-50 µm depending on the needle size, type and the roughness of the substrate used for printing. For the trace cross-section and width measurement work, needle tip diameter was varied from 14 gauge (1.54 mm inner diameter) to 30 gauge (0.15 mm inner diameter) along with the needle type (stainless steel vs. polypropylene) with most of the samples made with a 22 gauge polypropylene cone-shaped needle tip. To measure the average width, a test pattern was printed consisting of a series of 5 straight parallel lines separated by 1 mm and

having a length of 30 mm each. The entire process was imaged and recorded using a 10x macro zoom lens from Edmund Optics, Inc. The final setup looks something as shown in **Figure S1**. The G-codes for printing various patterns were first made using Corel Draw and then converted into G-code using a software called VCarve from Vectric Systems, Inc. The incision process for making inlet and outlet in microchannels was made using a Miltex biopsy punch with plunger from Ted Pella, Inc. The liquid metal EGaIn (99.99% pure) was purchased directly from Indium Corporation, Inc.

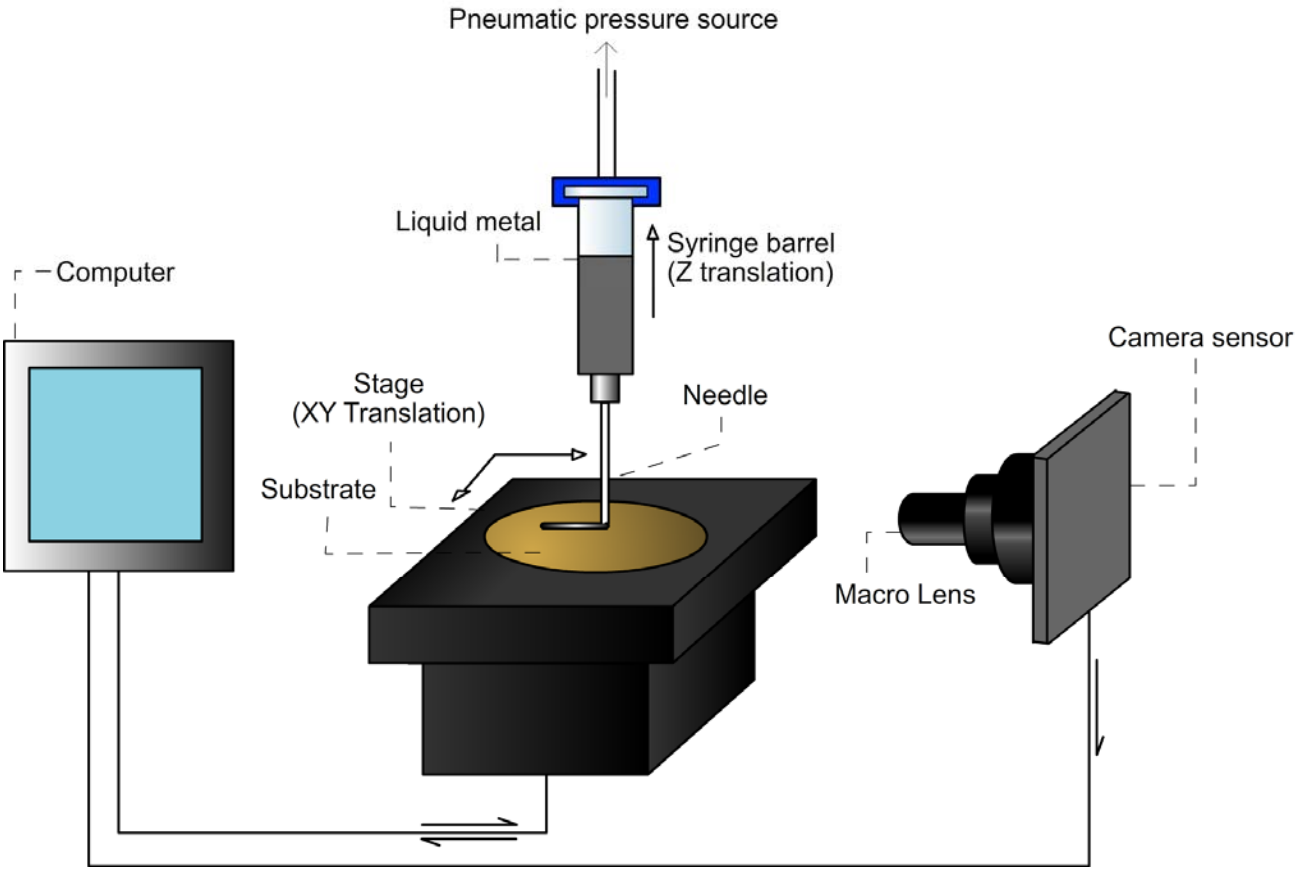

Figure S1. Experimental setup for 3D printing with liquid metals.

Substrates. Microscopic glass slides were purchased from Dow Corning, Inc. and were pretreated with a UVO plasma machine for 20 minutes to burn off all the surfactants on the glass

surface. PDMS surfaces were made using a SYLGARD® 184 silicone elastomer kit from Dow Corning, Inc. and were cured in a petri dishes at room temperature overnight. A kit of photocurable glues was purchased from Norland Optical Adhesives (NOA) and cured using an IntelliRay UV flood curing system.

Line Roughness Measurements. The geometry of the printed liquid metal traces was measured using an optical microscope with representative images as shown in **Figure S2**. To observe the uniformity on a macroscopic scale, we printed 10 lines each of 60 mm in length separated by 1 mm from each other on a glass slide pre-treated with UV-ozone for 20 minutes. The sample was then imaged using a stereoscope as shown in **Figure S2a**. The resulting lines were smooth and uniform at this length scale across the substrate.

Line width roughness (LWR) is the deviation in the line width measured over a given length of the line feature (Reference: Cao, H. B. *et al.* Sources of line-width roughness for EUV resists. in SPIE Proceedings 5376, Advances in Resist Technology and Processing, 757–764). We use LWR as a metric to determine the uniformity of the wire diameter. To measure LWR, we printed five lines, each 3 cm in length using a variety of needle gauges on a PDMS substrate and then imaged them using an optical microscope as shown in **Figure S2b**. The same images were then analyzed with an edge detection script written using MATLAB to threshold and help capture the profile of the line as shown in the right image in **Figure S2c**. The same MATLAB program also allowed us to split the image into pixels and hence measure the line width across each image using a data set of 2496 points per image. The 'error bars' on the data plotted in Figure 2b in the manuscript report the standard deviation among five samples. For example, a needle with a 410 μm inner diameter produces features with a standard deviation of ~7 μm. The LWR increases

with larger needle diameters, although there are likely many factors that could affect the quality of the printing beyond needle diameter.

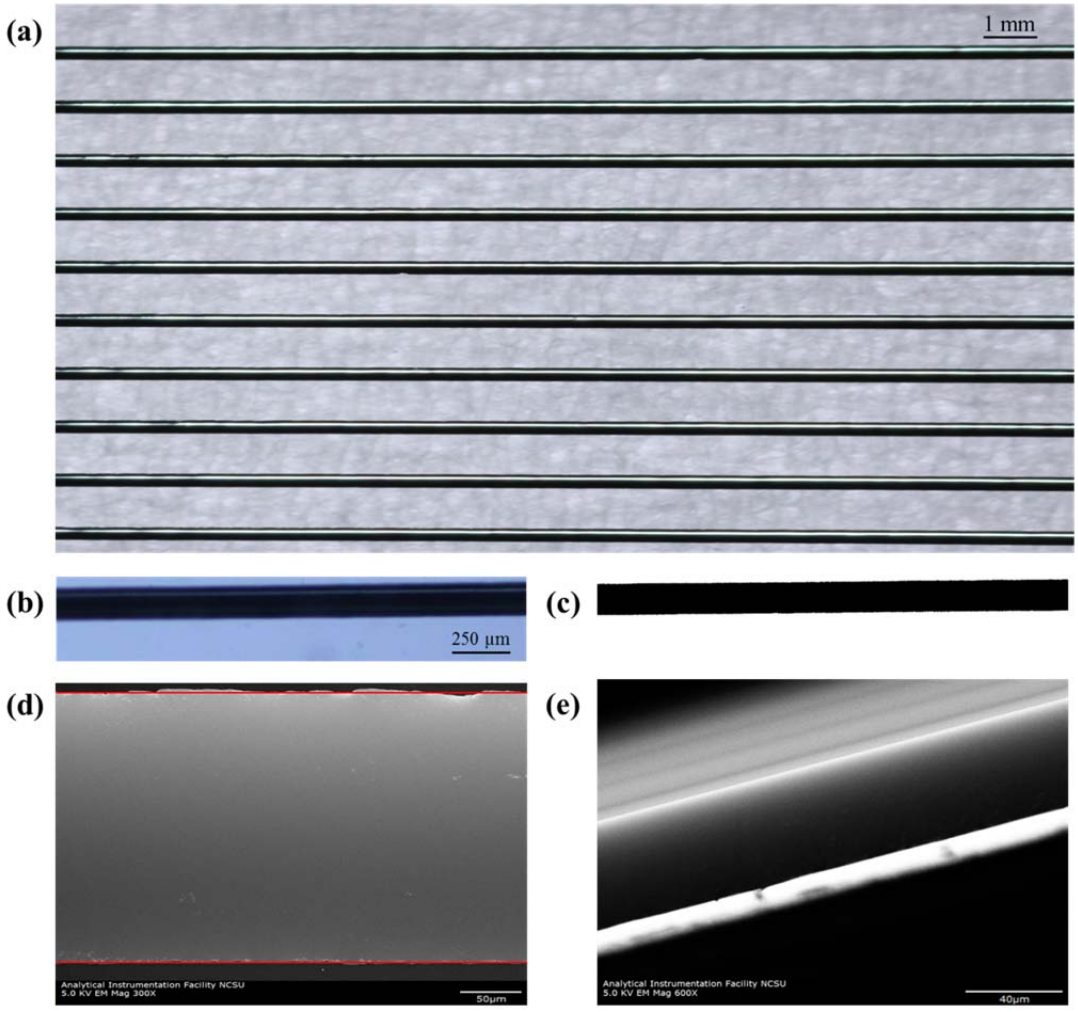

Figure S2. (a) Optical microscope image of ten liquid metal lines printed on a glass slide with each line 60 mm long, separated by 1 mm. (b-c) Optical microscope image (b) and grayscale threshold image (c) of a representative printed line for line width measurements. (d-e) SEM images of a printed line on a Si wafer for LER (d) and LHR (e) measurements. The stage is tilted in the image in (e), which provides a side view of the printed liquid metal.

Line edge roughness (LER) is defined as the deviation of a feature edge when viewed top-down from a microscope as compared to a smooth and ideal shape. Usually, the feature edge deviations observed are on a scale much smaller than the resolution limit of the imaging device used to pattern or print that feature (Reference: Chris A. Mack, Fundamental Principles of Optical Lithography: The Science of Microfabrication, John Wiley & Sons). To estimate LER, we used 10 lines printed on a silicon wafer and imaged them using a SEM. Two straight lines were provided to guide the eye and to offer a reference point to measure deviations from ideality. We took 20 equally spaced points on both the line edges and averaged the deviation from the red line (**Figure S2d**). The LER is not the same for both sides of the line. The LER for the top of the line averages to ~2.9 μm with a ~0.9 μm standard deviation. The LER for the bottom of the line averages to ~1.55 μm with a standard deviation of ~0.32 μm. The SEM used in the analysis was a Hitachi S3200N variable pressure scanning electron microscope (VPSEM). We neglect any uncertainty from the SEM due to the large size of the features.

Finally, we estimate the variation in the height of the printed lines which we define as the line height roughness (LHR). For this work, we used the same lines printed from **Figure S2a** as well as a liquid metal trace printed with a 1.36 mm inside diameter needle (15 gauge) on PDMS. We used an optical microscope to estimate the channel height by measuring the change in focal plane from the top to the bottom of the channels. Overall, 13 equally spaced measurements were taken on the samples along the length of the traces. We observed that the LHR (i.e. the standard deviation) was ~5 μm for a line printed with a needle of 410 μm inside diameter (5 μm is approximately the uncertainty with this crude measurement). With a 1.36 mm diameter needle, the LHR increased to ~25 μm. The absolute height of the printed lines were ~40 μm for the 410 μm needle and ~400 μm for the 1.36 mm diameter needle, indicating an increase in height with

increasing needle diameter. The observations were complimented by an SEM image as shown in **Figure S2e**. The image was obtained by tilting the sample holder of the VPSEM to ~70 degrees. The image confirms that the absolute height of the liquid metal line remains smooth and consistent over local length scales. In addition, the SEM images show that the surfaces of the metal structures are very smooth, as expected.

Electrochemical Withdrawal. A Keithley 2400 SourceMeter® was used for the liquid metal withdrawal from microchannels. The electrolyte used was 1M NaF in case of PDMS. The electrochemical parameters used in the process vary depending on the width and the length of the channel along with type of the casting polymer used in the process. In case of a photocurable glue like NOA, the constant current procedure was used with 50 μA in a solution of saturated NaF (5M) where we used platinum as the electrodes to avoid any corrosion / wetting problems with copper.

Inlet and Outlet Ports for a Microfluidic Device. As mentioned in the text, we can we can print microchannels with separate inlet and outlet ports that are made using liquid metal droplets on the drawn architecture as shown in **Figure S3**. The drop size is can be varied easily and hence can be made to stick out from the pattern even when it is completely embedded. The stable ports are beneficial as they remove an important step from the traditional microfluidic device fabrication process allowing easy interfacing of the conductive port with an external electrode (e.g., copper wire) in case of various lab-on-a-chip applications.

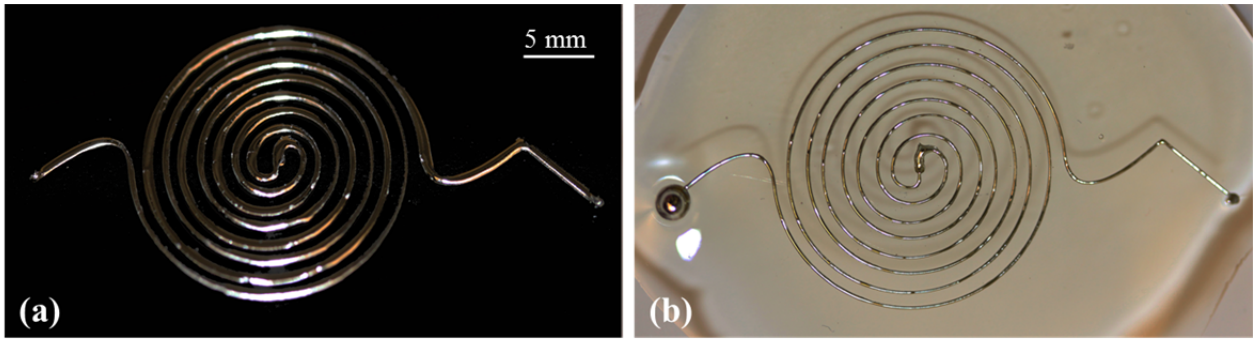

Figure S3. Printing Inlet and Outlet Port for a Microchannel for External Interfacing. Images of (a) A double spiral printed on an oxidized glass slide and (b) Liquid metal droplet of varying sizes printed at the start and the end of the microchannel that can be used as external ports for sensing applications.

Embedding Inlets and Outlets of the Microchannel. Every print pattern with a pillar in the Z-direction has to be partially embedded before it can be fully embedded to make the final microchannel. **Figure S4** depicts the process where we have a line ending with a vertical posts on each end that is stabilized first before curing the entire microchannel to make a monolithic structure shown in **Figure 6c, f** in the paper.

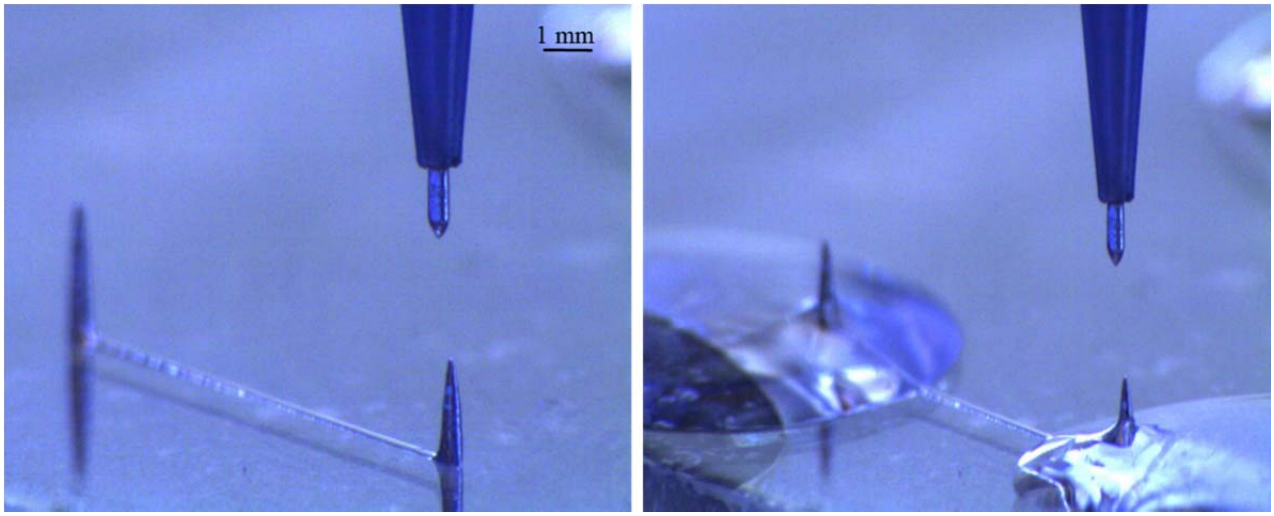

Figure S4. Embedding Inlets and Outlets of a Microchannel. Images of two 3D printed pillars of liquid metal connected by a straight 2D line and then encapsulated in photocured NOA-63 prepolymer.

Process Limitations. Some of the microvascular channels did not clean us uniformly with either the HCl flushing or the electrochemical withdrawal technique. We speculate that the bonding of the oxide skin to the surrounding polymer may explain this non-uniform withdrawal behavior. We are currently seeking to understand the conditions that cause this poor withdrawal. In some cases, the removal of the oxide appears to cause instabilities in the metal, which causes it to break up into metal droplets (**Figure S5 a & b**) or plugs (**Figure S5 c & d**).

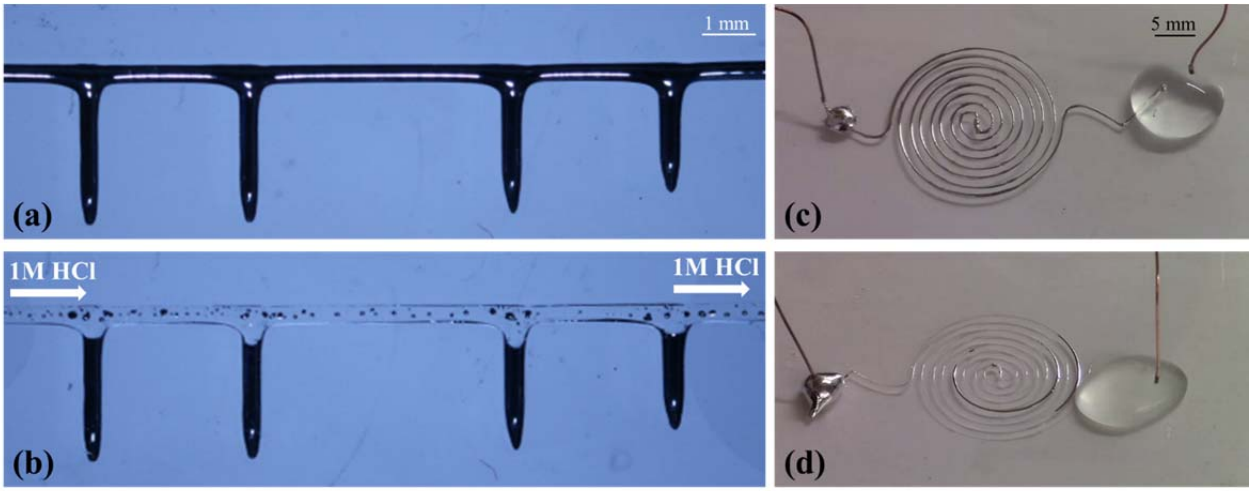

Figure S5. Incomplete withdrawal. (a-b) Images showing channels printed on and embedded in PDMS in which liquid metal residue remains after flushing with 1M HCl from left to right. (c-d) Images showing a double spiral printed on and embedded in NOA-63 where liquid metal traces remain while cleaning the channels via electrochemical withdrawal in a 5M NaF solution.